# Origin and function of the stalk-cell vacuole in *Dictyostelium*

Toru Uchikawa[a], Akitsugu Yamamoto[b], Kei Inouye[a]*

[a]Department of Botany, Graduate School of Science, Kyoto University
Sakyo-ku, Kyoto 606-8502, Japan
[b]Faculty of Bioscience, Nagahama Institute of Bio-Science and Technology
Nagahama, Shiga 526-0829, Japan

## Abstract

Large vacuoles are characteristic of plant and fungal cells, and their origin has long attracted interest. The cellular slime mould provides a unique opportunity to study the de novo formation of vacuoles because, in its life cycle, a subset of the highly motile animal-like cells (prestalk cells) rapidly develop a single large vacuole and cellulosic cell wall to become plant-like cells (stalk cells). Here we describe the origin and process of vacuole formation using live-imaging of *Dictyostelium* cells expressing GFP-tagged ammonium transporter A (AmtA-GFP), which was found to reside on the membrane of stalk-cell vacuoles. We show that stalk-cell vacuoles originate from acidic vesicles and autophagosomes, which fuse to form autolysosomes. Their repeated fusion and expansion accompanied by concomitant cell wall formation enables the stalk cells to rapidly develop turgor pressure necessary to make the rigid stalk to hold the spores aloft. Contractile vacuoles, which are rich in $H^+$-ATPase as in plant vacuoles, remained separate from these vacuoles. We further argue that AmtA may play an important role in the control of stalk-cell differentiation by modulating the pH of autolysosomes.

* Corresponding author. Fax: +81 75 753 4137.
E-mail address: inoue@cosmos.bot.kyoto-u.ac.jp (K. Inouye).

## Introduction

*Dictyostelium* is one of the simplest multicellular organisms, which has both animal-like and plant- or fungus-like characteristics in its life cycle; amoeboid cells aggregate to form a multicellular structure called a slug, which migrates and eventually forms a fruiting body consisting of a mass of spores held aloft by a stalk. Since the stalk is the backbone that determines the basic structure of the fruiting body of all dictyostelid slime moulds, the mechanism of stalk formation is an interesting question from both developmental and evolutionary points of view.

During the formation of a fruiting body, a subset of the highly motile animal-like cells (prestalk cells) rapidly develop a single large vacuole and cellulosic cell wall to become plant-like cells (stalk cells). These distinctive features of stalk cells must be to meet the requirements to shape and make the stalk suitable for supporting the spores with the minimum sacrifice of stalk cells. A number of studies have focused on the initiation of stalk cell differentiation, and a polyketide-derived morphogen DIF-1 and several transcription factors, such as DimA, DimB, MybE have been identified that regulate early steps of stalk cell differentiation (for a review, Williams, 2006). The later steps of stalk cell differentiation require activation of cAMP-dependent protein kinase (PKA) (Harwood et al., 1992), and are suppressed by ammonia (Schindler and Sussman, 1977). Singleton et al. (1998) showed that the PKA activation is negatively regulated by the DhkC phosphorelay signal transduction pathway. They further showed the involvement of ammonium transporters in the regulation of fruiting body formation. *Dictyostelium discoideum* has five Amt/Mep/Rh genes (Yoshino et al., 2007) and among these, AmtA and AmtC are proposed to regulate the initiation of fruiting (Singleton et al., 2006; Kirsten et al., 2005). On the other hand, Gross and coworkers showed that the effects of ammonia are mediated by elevation of the pH of acidic compartments (Davies et al., 1996), and proposed a mechanism involving $Ca^{2+}$ sequestration by a $Ca^{2+}/H^{+}$ exchanger in these compartments for the downstream regulation (Rooney and Gross, 1992; Gross, 2009).

In contrast, our knowledge of the morphological and structural changes associated with stalk cell differentiation is limited. Electron microscopic studies have shown that stalk-cell vacuoles contain mitochondria and other cellular material, and this has been taken to indicate that stalk cell vacuoles originate from autophagic vacuoles (autolysosomes) (Maeda and Takeuchi, 1969; George et al., 1972; Tang et al., 2006), which are particularly conspicuous in prestalk cells (MacWilliams and Bonner, 1979; Yamamoto, et al., 1981). Several atg genes have been identified in *Dictyostelium*, and

their mutants show varying degrees of autophagy defects (Otto et al., 2003; 2004; Tekinay et al., 2006). On the other hand, observation of stalk cells differentiating in monolayer conditions in the presence of DIF-1 or 8-Br-cAMP (a permeant analogue of cAMP that can activate PKA) showed that stalk cell differentiation proceeds in the order of loss of cell motility, vacuole enlargement, and cell wall formation (Kubohara et al. 1993; Levraud et al. 2003). However, the changes in the subcellular structures have not been studied in detail, and it remains unknown how these changes are related to the molecular mechanisms regulating the differentiation of stalk cells.

As a step to filling this gap, we focused on the stalk-cell vacuole, and have been trying to answer such questions as to where it comes from, how it grows, why it is controlled by ammonia, and what functions it may have for the generation of the adaptive features of stalk cells. Such a study has been hindered by the lack of membrane markers of the stalk-cell vacuole. Although neutral red and other basic dyes have been widely used as a marker of autophagic vacuoles, they are not suitable for tracing the process of its formation. We searched for molecules that are not only present on the membrane of stalk cell vacuoles but also likely to play important roles in the control of stalk cell differentiation. We speculated that one of the *Dictyostelium* ammonium transporters, AmtA, may be a candidate, since the target of the ammonia inhibition of stalk cell differentiation is acidic compartments including the stalk-cell vacuole (Davies et al., 1993), and since AmtA was reported to be enriched in prestalk cells with its lack causing early differentiation of stalk cells (Follstaedt et al., 2003; Singleton et al., 2006; but see Yoshino et al., 2007). We also developed a method for high-magnification live-imaging of the process of stalk cell differentiation in normal morphogenesis, and used it to verify the results obtained in monolayer experiments.

This study has another interesting aspect. Although the central vacuole of plant cells is indeed central to various aspects of plant cell activities, the process of its generation and development has not been well documented *in vivo*, because observation of its *de novo* formation in living tissues is very difficult and because many plant cultured cell lines inherit vacuoles from mother cells. As *Dictyostelium* is believed to have diverged from the animal/fungal lineage relatively soon after the divergence of the plant branch (Baldauf and Doolittle, 1997; Eichinger et al., 2005), understanding of the mechanism of the formation of stalk-cell vacuoles in *Dictyostelium* may provide some insight into the ontogenetic and phylogenetic origins of the vacuoles.

## Materials and methods

### Cell growth, staining, starvation and development

*Dictyostelium discoideum* strain Ax2 and its derivatives were used in this study. Cells were grown in HL5 medium (Watts and Ashworth, 1970) without (Ax2) or with 20 μ g/ml G418 (AmtA-GFP, GFP-Atg8, GFP-Rab11), 50 μ g/ml hygromycin (GFP-VatM), or 4 μ g/ml blasticidin (RFP-Atg8) at 22C in shaking culture or in petri dishes in the dark. For starvation, cells were washed twice and shaken in 20 mM $KK_2$ phosphate buffer (pH 6.0) typically for 6-8 hours in flasks. For development, washed cells were streaked or spotted on 1.5% agar dissolved in distilled water or phosphate buffer. Slugs obtained after 16-20 hours were used for observation or dissociation.

For vital staining, washed vegetative cells were incubated in 0.005% neutral red, 50 μ M LysoTracker Red in phosphate buffer for 5 minutes at 0C and washed twice in phosphate buffer by repeated centrifugation. For cell wall detection, dissociated prestalk cells were incubated in the presence of 0.001% Calcofluor. For TRITC-dextran introduction, TRITC-dextran were introduced into washed vegetative cells suspended in ice-cold 20 mM $KNa_2$ phosphate buffer, pH 7.4 containing 2mM $MgCl_2$, 0.2 mM $CaCl_2$, 50 mM sucrose by electroporation, and the cells were incubated for 5 minutes on ice and washed twice in the same buffer by repeated centrifugation.

### Fusion constructs

The GFP-Rab11 and GFP-VatM plasmids were kindly provided by Dr. K. Yoshida (Harris et al., 2001; Heuser et al., 1993). The RFP-Atg8 plasmids were obtained from dictyBase stock center (http://dictybase.org/StockCenter/StockCenter.html). The coding region of AmtA was obtained by reverse-transcription of an RNA sample from starved Ax2 cells and PCR-amplification using a primer pair TTAAGCTTATGGTAGCAGGAGAAATAATAAAAGG and GGGGTACCTTTAAAAAAATCATGACTATTAATAACAGATG which contain in-frame artificial HindIII (5'-) and KpnI (3'-) reaction sites, respectively, and ligated into pDXA-GFP2 (Levi et al., 2000) at the C-terminal side of GFP under the control of the constitutive actin15 promoter. The correct insertion was confirmed by sequencing and named "AmtA-GFP". The coding region of Atg8 was also obtained with primer pair GAGCTCATGGTTCATGTATCAAGCTT containing in-frame artificial SacI (5'-) reaction site and GGCAAACTATTATTGTTTGCA, and ligated into the pCR 2.1 vector (Invitrogen), digested with SacI and ligated into pDXA-GFP2 at the N-terminal side of GFP. The correct insertion was confirmed by sequencing and named "GFP-Atg8". The GFP or RFP constructs were introduced into Ax2 cells by electroporation, and transformants were selected for resistance to hygromycin (GFP-VatM), blasticidin

(RFP-Atg8) or G418 (all others).

**Prestalk cell isolation and agar-overlay method**

To obtain dissociated prestalk cells, anterior part of 16-20 hour slugs was cut and collected in buffer (20 mM phosphate buffer, 1 mM EDTA, 0.1 mM cAMP). The slugs were dissociated into single cells by repeated passages through a 26G needle with a 1 ml syringe (Inouye and Gross, 1993). To induce stalk cell differentiation in monolayer, isolated prestalk cells ($1\times10^3$-$1\times10^4$ cells/$cm^3$) were washed twice with phosphate buffer and incubated with stalk salts (10 mM KCl, 2 mM NaCl, 1 mM $CaCl_2$, 10 mM MES-KOH, pH 6.2) supplemented with 10 mM 8-Br-cAMP on a coverslip (Brookman et al., 1982). To observe cells in detail, the agar-overlay method (Fukui et al., 1987) was performed with minor modifications; 10 mg of agarose was dissolved in 1 ml of phosphate buffer or stalk salts containing 10 mM 8-Br-cAMP and placed on a tissue culture dish. A piece of agarose sheet (~0.8 mm thick) was placed on the cells attached to the coverslip, and excessive buffer was removed from the periphery of the agarose sheet using a Pasteur pipet and pieces of filter paper.

**Microscopy**

Confocal images were taken with a Zeiss LSM510 confocal microscope using a 20× 0.50 N.A. Plan-Neofluar objective lens or 63× 1.4 NA Plan-Apochromat oil-immersion lens. For GFP, the 488 nm line of the argon laser was used with a 500-530 nm emission filter. For RFP, neutral red, LysoTracker Red and TRITC, the HeNe 543 nm laser was used with a 560 nm long-pass emission filter. For simultaneous recording of vacuole development and cell wall formation, a NIKON TMD inverted microscope with a 40× phase-contrast objective was used. Image J (developed at the US National Institutes of Health and available at http://rsb.info.nih.gov/nih-image/) was used for all data analysis. To obtain confocal image of cells during fruiting body formation at high magnification, a piece of agar plate carrying elongating fruiting bodies was cut out and placed in a shallow well made of a glass slide and a silicone rubber spacer with a thickness that is slightly larger than the agar. Fruiting bodies were immediately immersed in a drop of liquid paraffin (Nacalai tasque) and covered with a coverslip in such a way that the sorogen would come close to the coverslip but stay apart from the agar. Under this condition, the stalk continued elongation and spores differentiated at some point.

**Immunoelectron microscopy**

The pre-embedding gold enhancement immunogold method was performed as previously described (Hayashi-Nishino et al., 2009) with a slight modification. In brief, starved cells attached on coverslips were fixed in $KK_2$ phosphate buffer containing 2% paraformaldehyde and 0.05% glutaraldehyde for 60 minutes at room temperature. Cells were permeabilised in cold methanol for 10 min at -20C. After washing in 0.1 M sodium phosphate buffer at pH 7.4 (PB), the cells were blocked for 30 min in PB containing 0.1% saponin, 10% bovine serum albumin, 10% normal goat serum, and 0.1% cold water fish skin gelatin, and then exposed overnight to rabbit anti-GFP polyclonal antibody (a gift of Dr. N. Nakamura) in a blocking solution. The specimens were incubated with colloidal gold (1.4 nm in diameter, Nanoprobes)-conjugated goat anti-rabbit IgG in blocking solution for 2 h, and the signal was intensified with a gold enhancement kit (GoldEnhance EM, Nanoprobes) for 5 min at room temperature. The specimens were post-fixed in 1% OsO4 containing 1.5% potassium ferrocyanide, then dehydrated in a series of graded ethanol solutions and embedded in epoxy resin. Ultra-thin sections were collected and stained with uranyl acetate and lead citrate, and observed under a Hitachi H7600 transmission electron microscope.

**Reagents and growth media**

Bacto-pepton, yeast extract, and bacto-agar were purchased from Difco Labolatories (Detroit, MI, USA). Neutral red, TRITC-dextran, hygromycin, cAMP sodium salt and 8-Br-cAMP were from Sigma Chemical Company (St. Louis, MO, USA). Lyso Tracker Red was from Invitrogen (Carlsbad, California, USA). Other standard media components were from Nacalai tesque (Kyoto, Japan), Waken (Kyoto, Japan) or Wako (Osaka, Japan).

## Results

### AmtA-GFP can be used as a marker for stalk-cell vacuole membranes to study the origin of the stalk-cell vacuole

An AmtA-GFP fusion gene was constructed under the control of the constitutive actin 15 promoter and introduced into Ax2 cells. Transformed cells (AmtA-GFP cells hereafter) grew normally, and in vegetative cells, AmtA-GFP was localised to endo-lysosomal membranes, endoplasmic reticulum membranes and nuclear envelope, but virtually undetectable on the plasma membrane and contractile vacuole membranes

(not shown). These results largely agree with the results of Kirsten et al. (2008). AmtA-GFP cells developed normally to produce proportionate fruiting bodies, in which GFP fluorescence was predominantly localised on the membrane of large vacuoles in stalk cells within the stalk tube (Fig. 1A arrowheads) and of smaller vesicles in prestalk cells. Live-tissue imaging of forming fruiting bodies indicated that small vesicles with GFP fluorescence in prestalk cells fused to form large vacuoles after the cells entered the stalk tube (Fig. 1B). Stalk cell differentiation can also be induced *in vitro* by adding 8-Br-cAMP to dissociated prestalk cells in submerged culture (Maeda, 1988). In stalk cells differentiating *in vitro*, AmtA-GFP was mainly located on the membrane of stalk-cell vacuoles, while weak fluorescence was also detected on the nuclear envelope (Fig. 1C arrowheads). Time lapse movies demonstrated repeated fusion of AmtA-GFP vesicles to form a large vacuole during stalk cell differentiation (Fig. 1D, Movie 1). No GFP-negative vesicles that were visible with transmitted light have been observed to fuse with the growing stalk-cell vacuoles (not shown). Estimates of the surface areas of the AmtA-GFP vesicles indicate that the sum of the surface areas of the smaller vesicles is roughly equal to the surface area of the resulting larger vesicles at every fusion event, indicating that these vesicles are at least the major sources of the membrane of stalk-cell vacuoles (Fig. 1E). These results strongly suggest that the stalk-cell vacuole does not form by steady expansion of a stalk-cell vacuole precursor but in a series of fusion of large AmtA-GFP vesicles. We therefore used in the following experiments the AmtA-GFP fluorescence as a marker to study the formation of stalk-cell vacuoles.

**Autolysosomes strongly contribute to the stalk-cell vacuole**

In *Dictyostelium*, as in many other types of cells, starvation induces autophagy and promotes autophagosome formation (Kosta et al, 2004), if the cell density is high enough to allow cell communication (Yamamoto et al., 1981). Intracellular membrane-bound structures containing mitochondria or cytosol may therefore be interpreted to be autophagosomes or autolysosomes if they are induced under starvation conditions. Electron microscopic studies of starved *Dictyostelium* cells have demonstrated the presence of autophagosomes/autolysosomes containing organelles such as mitochondria (Maeda and Takeuchi, 1969; George et al. 1972, Tang et al. 2006). We performed immuno-electron microscopy of AmtA-GFP cells using an anti-GFP antibody and colloidal gold conjugates (Fig. 2A), and found that in starved cells the membrane of some vacuoles was decorated with gold particles, and that many of these vacuoles contained structures that are most likely mitochondria (magenta arrows). Some of these vacuoles (magenta arrowhead) were filled with undigested mitochondria, while larger ones (green arrowhead) were mostly electron-lucent,

suggesting that the former are autophagosomes and the latter are autolysosomes.

As a cytosol marker, we used tetramethylrhodamine-conjugated dextran (TRITC-dextran), which does not readily cross the cell membrane or organelle membranes. TRITC-dextran was introduced into the cytosol of AmtA-GFP cells by electroporation and the cells were transferred to starvation conditions. Right after loading, rhodamine fluorescence was spread all over the cytosol but not in organelles (Fig. 2B top). After starvation, rhodamine fluorescence was detected in most AmtA-GFP vesicles and the fluorescence level of the cytosol decreased (Fig. 2B centre). All rhodamine-patches were surrounded by GFP fluorescence. It was also noted that some AmtA-GFP vesicles, mostly small ones, were without detectable rhodamine fluorescence (Fig. 2B arrows). In non-starved control cells, the level of rhodamine fluorescence in the cytosol was higher, whereas AmtA-GFP vesicles containing rhodamine fluorescence were much fewer, than those under starvation conditions (Fig. 2B bottom), indicating that much of the translocation of TRITC-dextran from the cytosol into AmtA-GFP vesicles is a starvation-dependent process. Similar concentration of cytosolic fluorescent dextran by autophagy has been shown to occur in mammalian cells (Hendil, 1981; Hariri et al., 2000; Larsen and Sulzer, 2002). In prestalk cells, rhodamine fluorescence remained concentrated in AmtA-GFP vesicles, but in stalk cells, it was diminished in the stalk-cell vacuoles (data not shown), presumably due to degradation of the probe within these vacuoles, which are very acidic (Kay et al., 1986).

The above results suggest the involvement of AmtA-GFP vesicles in autophagy. In animal cells as well as plant/fungal cells, autophagosomes fuse with lysosomes to form autolysosomes. To see whether AmtA-GFP vesicles are acidic or not, AmtA-GFP cells were loaded with an acidotropic probe neutral red and examined at various times of starvation using a confocal microscope. In starved AmtA-GFP cells, red fluorescence of neutral red was detected only within AmtA-GFP vesicles, while a small number of AmtA-GFP vesicles were devoid of the probe (Fig. 2C arrow), indicating that all acidic vesicles detectable with this method have AmtA-GFP on their membranes and that there are also AmtA-GFP vesicles that are not acidic. Experiments using another acidotropic probe LysoTracker gave essentially identical results (not shown). Acidic AmtA-GFP vesicles that do not take up the cytosolic fluorescent dextran will be acidic organelles, possibly lysosomes.

The results that most AmtA-GFP vesicles took up the cytoplasmic fluorescent dextran and that most AmtA-GFP vesicles were acidic indicate that the majority of AmtA-GFP

vesicles are autolysosomes. To verify that AmtA-GFP is present on autophagosome membranes, as suggested by immuno-electron microscopy, we used Atg8 as a marker of autophagosomes. Atg8 is a ubiquitin-like protein involved in the formation of autophagosomes in yeast (Kirisako et al., 1999; Levine and Klionsky, 2004), and its *Dictyostelium* orthologue was reported to be localised to preautophagosomal complexes or autophagosomes, as in many other types of cells (Otto et al., 2003; 2004). An N-terminal GFP-fusion construct of Atg8 was made and introduced into Ax2 cells, and simultaneous staining with neutral red was performed in the same way as shown above (Fig. 2D). There was no overlap between GFP-Atg8 and neutral red fluorescence, suggesting that Atg8 is located on (pre)autophagosome structures but no longer present on the autolysosome membranes. As with the case of the yeast autophagic pathway (Levine and Klionsky, 2004), Atg8 in *Dictyostelium* is probably degraded or reused for de novo formation of autophagosomes. RFP-Atg8 (Tekinay et al., 2006) was introduced into AmtA-GFP-expressing cells and their spatial relationship was examined after starvation (Fig. 2E). As RFP tended to aggregate after extended period of incubation, cells starved for a shorter period and showing similar distribution patterns as GFP-Atg8 were used. As shown in Fig. 2E, some of the AmtA-GFP vesicles were colocalised with RFP-Atg8. These results together suggest that a small fraction of AmtA-GFP vesicles are in fact autophagosomes.

Throughout development, GFP-Atg8 was present on small vesicles alone (Fig. 3A). In stalk cells, GFP-Atg8 was also located on the membranes of autophagosomes but absent from the membrane of stalk-cell vacuoles (Fig. 3A), suggesting that autophagy is still active in differentiating stalk cells. This is also supported by time-lapse movies of differentiating stalk cells in monolayer culture (Fig. 3B, Movie 2). Autolysosomes, on the other hand, increase in size over the course of development (Yamamoto and Takeuchi, 1983), presumably due to fusion of newly formed autophagosomes with existing autolysosomes. When prespore and prestalk cells differentiate, autolysosomes in prestalk cells grow in size (Yamamoto et al., 1981), whereas in prespore cells, they remain small and become less acidic (Yamamoto and Takeuchi, 1983), and when stalk cell differentiation is induced, they rapidly fused, as shown in Fig. 1.

**The contractile vacuole is distinct from the stalk-cell vacuole**

Possible involvement of contractile vacuoles in the formation of stalk-cell vacuoles was investigated, since both organelles are capable of accumulating water and since vacuolar $H^+$-ATPase, which is predominantly located on vacuole membranes in plants, is abundant on the membranes of contractile vacuoles in *Dictyostelium* (Fok et al., 1993; Nolta et al., 1994; Bush et al., 1994). Kirsten et al. (2008) showed that AmtA is

absent from the contractile vacuole in growth phase cells, and we confirmed this to be the case in starved cells as well. We investigated the behaviour of contractile vacuoles in differentiating stalk cells in monolayer culture and in normal development using GFP-Rab11 and GFP-VatM. VatM is the 100 kDa subunit of the vacuolar $H^+$-ATPase, which is mainly located on contractile vacuole membranes and to a 10-fold lesser extent on endo-lysosomal membranes in *Dictyostelium* (Clarke et al., 2002), whereas Rab11 is almost exclusively localised to contractile vacuole membranes (Harris et al., 2001). Fig. 3C shows selected frames from a time-lapse recording of a differentiating stalk cell expressing GFP-Rab11 in monolayer culture. Contractile vacuoles remained active throughout the period, and there was no indication of the GFP-fluorescence to translocate to the membrane of developing stalk-cell vacuoles (Movie 3). In differentiating stalk cells within the stalk tube and in basal disk of a fruiting body also, contractile vacuoles appeared to be functioning within the limited space of the remaining cytoplasm independently of the stalk-cell vacuole. Essentially identical results were obtained when GFP-VatM was used as a marker (Figs 3D,E arrows, Movies 4,5), except that GFP-VatM was also present on the membrane of stalk-cell vacuoles (Fig. 3E arrowheads), as would be expected if they are partially derived from lysosomes and capable of maintaining low internal pH.

**The expansion of the stalk-cell vacuole is restricted by the cell wall**

Even after the final fusion of major vacuoles to form a single stalk-cell vacuole, its expansion continued for several hours, while the rate of volume increase of the vacuole and the entire cell gradually slowed down (Fig. 4). One possible cause of this cessation of vacuole and cell expansion will be the cell wall. Like plant and fungal cells, stalk cells form cell walls. We investigated the relationship between the development of stalk-cell vacuole and cell wall formation. Observation of differentiating stalk cells *in vitro* in the presence of Calcofluor as a cell wall marker revealed that the rate of stalk-cell vacuole expansion decreased as the cell wall began to be formed (Fig. 5, Movie 6), suggesting that the slowing down of vacuole volume may be caused by the developing cell wall restricting cell expansion.

## Discussion

We have shown that stalk-cell vacuoles are made from vesicles carrying AmtA on their membranes in prestalk cells. These vesicles were identified to be autolysosomes

(autophagic vacuoles), confirming the earlier suggestion that stalk cell vacuoles are enlarged autophagic vacuoles (Maeda and Takeuchi, 1969; George et al., 1972; Tang et al., 2006). The involvement of autophagy in the formation of stalk-cell vacuoles suggest that autophagy mutants may have defects in the formation of stalk-cell vacuoles. Otto et al. have examined several *Dictyostelium atg* genes and showed that their mutants show varying degrees of defects in autophagy and development. Among these, the *atg1* mutant displays the most severe phenotype, lacking autophagy and being arrested at the mound stage in development (Otto et al., 2004). Under monolayer conditions, *atg1* mutant cells that are induced to differentiate into stalk cells by addition of DIF-1 do make cell walls but do not form large vacuoles (Kosta et al. 2004), consistent with the requirement of autophagy for the formation of stalk-cell vacuoles. The *atg5* and *atg7* mutants show reduced autophagy and, in development, proceed beyond the mound stage but are unable to form fruiting bodies (Otto et al. 2003), whereas the phenotype of the *atg6* and *atg8* mutants are mild and they form small fruiting bodies (Otto et al. 2004). Corresponding to the severity of autophagy defects of the mutants, the final multicellular structures of the *atg1* mutant completely lacked cells having large vacuoles, whereas the *atg5* and *atg7* mutants made only a small number of vacuolated stalk cells (our unpublished observations). The *atg6* and *atg8* mutants formed stalk cells containing a large stalk-cell vacuole and cell wall. These results suggest that the ability of the cells to form stalk-cell vacuoles are positively correlated with the activity of autophagy.

**Functions of the stalk-cell vacuole**

The rapid increase in the total vacuole volume and slow decrease in the cytosol volume (Fig. 4), together with the continuing presence of autophagosomes in differentiating stalk cells (Fig. 3B), suggests that degradation is still going on in stalk cell vacuoles. Our earlier results that ammonia removal induces vacuole acidification and stalk cell differentiation (Inouye, 1988a; 1988b) suggest that degradation in stalk-cell vacuoles proceeds at an even higher rate than in autolysosomes in prestalk cells, because the vacuolar pH of the stalk cells is lower than that of prestalk cells (Kay et al., 1986) and because lytic activity of vacuoles is higher at lower pH. This is in accord with the observation by Gregg et al. (1954) that a large amount of ammonia was released during fruiting body construction, and that the stalks of the fruiting bodies contained considerably larger amounts of non-protein nitrogen than spores or slugs. These results together indicate that degradation is an important function of the stalk-cell vacuole.

Degradation of macromolecules and organelles in the vacuoles, together with the transport of ions into the vacuoles driven or facilitated by the proton gradient, such as $Ca^{2+}$ influx by $Ca^{2+}/H^{+}$-ATPase (Gross, 2009), will lead to an increased osmotic pressure, which will in turn cause the influx of water into the vacuoles. The total volume of the vacuoles increases to the extent that they occupy a substantial portion of the cell and make the cell expand (Fig. 4). This indicates that a second important role of the stalk-cell vacuole is to expand the cell. The reason why small vacuoles fuse to form a single large vacuole (a stalk-cell vacuole) will be that it enables the vacuoles to substantially increase their total volume with a limited amount of vacuole membranes (Fig. 1F). For instance, the membranes of 100 small autolysosomes with a diameter of 1 μm are enough to make one large spherical vacuole with a diameter of 10 μm, which holds 10-times more water than they did initially.

In monolayer experiments, vacuole enlargement slowed down as the cell wall started to be formed (Fig. 5), suggesting that the cell wall is a factor limiting the expansion of stalk-cell vacuoles. Most probably, vacuole expansion and the resistive force by cell walls generate turgor pressure, providing higher mechanical strength than with cell walls alone (Klaus and George, 1974). Consistent with this, *Dictyostelium* cells lacking the single cellulose synthase gene (*dcsA*) and unable to make cell wall (Blanton et al., 2000), form larger stalk-cell vacuoles, and consequently become larger, than wild type cells (our unpublished observation). In normal morphogenesis, the final fusion of vacuoles to form a single stalk-cell vacuole occurs only in the stalk tube (Fig. 1B) where the cell wall is formed (Raper and Fennell, 1952; George et al., 1972; Grimson et al., 1996). This suggests that the fusion and enlargement of stalk-cell vacuole and the formation of the cell wall are under control to ensure the generation of turgor pressure in each prestalk cell.

In the confined space of the stalk tube, stalk cells enlarge and push each other while resisted by the rigid stalk tube except at its apical opening (Raper and Fennell, 1952). Expansion of stalk cells and the resistive force by the stalk tube would generate a large pressure within the stalk tube, like the turgor pressure within each stalk cell. The upward movement of differentiating stalk cells in the upper part of the stalk is a manifestation of this pressure (Raper and Fennel, 1952). This “turgor pressure” of the entire stalk will provide the stalk with additional mechanical strength and smooth overall shape.

The above four functions of the stalk-cell vacuoles, i.e. degradation, cell expansion, turgor pressure of individual stalk cells, and turgor pressure of the stalk, manifesting in

this order, converge to the construction of a rigid stalk to hold the spores aloft. The volume increase of stalk cells has an additional advantage of needing fewer of them for construction of a fruiting body, providing a large allocation for spores, which would be evolutionarily adaptive.

**Possible roles of AmtA**

Our finding that AmtA-GFP resides on autolysosome membranes provides some insight into how it may function. During morphogenesis, stalk cell differentiation is repressed until prestalk cells enter the stalk tube. Ammonia, which is produced in a large amount during morphogenesis (Gregg, 1954; Schindler and Sussman, 1977), plays an important role in the control of stalk cell differentiation, with high ammonia conditions repressing stalk cell differentiation and low ammonia inducing derepression (Schindler and Sussman, 1977; Inouye, 1988b; 1990). Singleton et al. (2006) proposed that AmtA is an ammonia sensor acting upstream of the DhkC phosphorelay which controls cAMP-dependent protein kinase A activity to regulate fruiting body formation, but it has not been shown how it senses ammonia and how its signal is transduced to the downstream pathway. Gross and coworkers showed that the effects of ammonia are mediated by the pH of acidic compartments possessing vacuolar $H^+$-ATPase (Davies et al., 1996). As the majority of acidic compartments in later development are autolysosomes (Yamamoto and Takeuchi, 1983), it is plausible that AmtA on their membranes plays a role in the control of stalk cell differentiation.

AmtA is a member of the Amt/Mep/Rh family of proteins with 11-transmembrane domains, and the best studied member of the family E. coli AmtB has an $NH_4^+$-binding site on its N-terminal periplasmic side and after deprotonation transports $NH_3$ to the C-terminal side (Khademi et al., 2004; Zheng et al., 2004). Since the N-terminus of *Dictyostelium* AmtA faces to the luminal side and C-terminus to the cytosol (Kirsten et al., 2008), the direction of transport by AmtA on autolysosome membranes is most likely from the lumen to the cytosol. Although it has not been shown whether the transported species is $NH_3$ (as in as E. coli AmtB) or $NH_3 + H^+$ (as in Arabidopsis Amt1) (Ludewig, 2006), the phenotype of the *amtA*-null mutant in late morphogenesis, i.e. earlier stalk cell differentiation (Singleton et al., 2006) suggests that it is $NH_3 + H^+$, because this phenotype is analogous to the effects of vacuole acidification (Fig. 6). If this is the case, AmtA would function as a conduit for ammonia as a proton carrier to prevent excessive acidification of autolysosomes in prestalk cells until challenged by low ammonia environments (Fig. 6). However, another null strain shows increased sensitivity to ammonia in earlier developmental stages (Yoshino et al., 2007) which is difficult to reconcile with the above model.

Further analysis of the *amtA* mutant will be necessary to clarify the role of the protein.

**Origin of large vacuoles**

In many plant cells, vacuoles are inconspicuous soon after cell division, but gradually develop to eventually occupy almost the entire cell volume. Electron microscopic observations of meristematic cells have indicated that vacuole formation involves autophagy, as well as compartmentalisation of the endoplasmic reticulum and trans-Golgi network (Marty, 1999; Maeshima et al., 2001). Autophagy is also implicated in the growth of vacuoles in filamentous fungi in which small vacuoles are inherited from mother cells (Shoji et al., 2006; Kikuma et al., 2006). The results of the present study show that the origin of the stalk-cell vacuole of *Dictyostelium* can be traced back to autophagosomes. Molecular phylogeny studies show that *Dictyostelium* and other slime moulds diverged from the animal-fungi lineage after the plant-animal split (Baldauf and Doolittle, 1997; Eichinger et al., 2005). The ability of making large vacuoles may have an ancient origin, possibly related with degradation of cellular components and, in conjunction with the cell wall, adding structural strength to the cells. In this context, it may be interesting to study the mechanism of vacuole formation in protozoans and unicellular algae that develop a large vacuole and cell wall at some point of their life cycle. As stalk cells of *Dictyostelium* are non-viable (Whittingham and Raper, 1960), they are unlikely to have some of the well-known functions of plant vacuoles, such as storage and toxic avoidance, which may be of independent origin.

**Acknowledgements**

T. U. was financially supported in part by the Global COE program A06 to Kyoto University. We thank Dr. K. Yoshida for providing the GFP-rab11A and GFP-VatM plasmids, help in the earlier phase of the work, critical comments on the manuscript, Dr. N. Nakamura for the rabbit anti-GFP polyclonal antibody and dictyBase for the RFP-Atg8 plasmid.

## References


Baldauf, S. L., Doolittle, W. F., 1997. Origin and evolution of the slime molds (Mycetozoa). Proc. Natl. Acad. Sci. USA 94, 12007-12012.

Becker, B., 2007. Function and evolution of the vacuolar compartment in green algae and land plants (Viridiplantae). Int. Rev. Cytol. 264, 1-24.

Blanton, R. L., Fuller, D., Iranfar, N., Grimson, M. J., Loomis, W. F., 2000. The cellulose synthase gene of *Dictyostelium*. Proc. Natl. Acad. Sci. USA 97, 2391-2396.

Brookman, J. J., Town, C. D., Jermyn, K. A., Kay, R. R., 1982. Developmental regulation of a stalk cell differentiation-inducing factor in *Dictyostelium discoideum*. Dev. Biol. 91, 191-196.

Bush, J., Nolta, K., Rodriguez-Paris, J., Kaufmann, N., O'Halloran, T., Ruscetti, T., Temesvari, L., Steck, T., Cardelli, J., 1994. A Rab4-like GTPase in *Dictyostelium discoideum* colocalizes with V-$H^+$-ATPase in reticular membranes of the contractile vacuole complex and in lysosomes. J. Cell Sci. 107, 2801-2812.

Clarke, M., Kohler, J., Heuser, J., Gerisch, G., 2002. Endosome fusion and microtubule- based dynamics in the early endocytic pathway of *Dictyostelium*. Traffic. 3, 791-800.

Davies, L., Satre, M., Martin, J. B., Gross, J. D., 1993. The target of ammonia action in *Dictyostelium*. Cell 75, 321-327.

Davies, L., Farrer, N. A., Satre, M., Dottin, R. P., Gross, J., 1996. Vacuolar $H^+$-ATPase and weak base action in *Dictyostelium*. Mol. Microbiol. 22, 119-126.

Eichinger, L., Pachebat, J. A., Glockner, G., Rajandream, M. A., Sucgang, R., Berriman, M., Song, J., Olsen, R., Szafranski, K. Xu, Q. et al., 2005. The genome of the social amoeba *Dictyostelium discoideum*. Nature 435, 43-57.

Fok, A. K., Clarke, M., Ma, L., Allen, R. D., 1993. Vacuolar $H^+$-ATPase of *Dictyostelium discoideum* - a monoclonal antibody study. J. Cell Sci. 106, 1103-1113.

Follstaedt, S. C., Kirsten, J. H., Singleton, C. K., 2003. Temporal and spatial expression of ammonium transporter genes during growth and development of *Dictiostelium discoideum*. Differentiation 71, 557-566.

Fukui, Y., Yumura, S., Yumura, T. K., 1987. Agar-overlay immunofluorescence: high-resolution studies of cytoskeletal components and their changes during chemotaxis.

Methods Cell Biol. 28, 347-356.

George, R. P., Albrecht, R. M., Raper, K. B., Sachs, I. B., Maclenxie, A. P., 1972. Scanning electron microscopy of spore germination in *Dictyostelium discoideum*. J. Bacteriol. 112, 1383-1386.

Gregg, J. H., Hackney, A. L., Krivanek, J. O., 1954. Nitrogen metabolism of the slime mold *Dictyostelium discoideum* during growth and morphogenesis. Biol. Bull. 107, 226-235.

Grimson, M. J., Haigler, C. H., Blanton, R. L., 1996. Cellulose microfibrils, cell motility, and plasma membrane protein organisation change in parallel during culmination in *Dictyostelium discoideum*. J. Cell Sci. 109, 3079-3087.

Gross, J. D., 1994. Developmental decisions in *Dictyostelium discoideum*. Microbiol. Rev. 58, 330-351.

Gross, J. D., 2009. Acidic $Ca^{2+}$ stores, excitability, and cell patterning in *Dictyostelium discoideum*. Eukaryot. Cell 8, 696-702.

Hariri, M., Millane, G., Guimond, M. P., Guay, G., Dennis, J. W., Nabi, I. R., 2000. Biogenesis of multilamellar bodies via autophagy. Mol. Biol. Cell 11,255-268.

Harris, E., Yoshida, K., Cardelli, J., Bush, J., 2001. Rab11-like GTPase associates with and regulates the structure and function of the contractile vacuole system in *Dictyostelium*. J. Cell Sci. 114. 3035-3045.

Harwood, A. J., Hopper, N. A., Simon, M. N., Bouzid, S., Veron, M., Williams, J. G., 1992. Multiple roles for cAMP-dependent protein kinase during *Dictyostelium development*. Dev. Biol. 149, 90-99.

Hayashi-Nishino, M., Fujita, N., Noda, T., Yamaguchi, A., Yoshimori, T., Yamamoto, A., 2009. A subdomain of the endoplasmic reticulum forms a cradle for autophagosome formation. Nat. Cell Biol. 11,1433-1437.

Hendil, K. B., 1981. Autophagy of metabolically inert substances injected into fibroblasts in culture. Exp. Cell Res. 135, 157-166.

Heuser, J., Zhu, Q., Clarke, M., 1993. Proton pumps populate the contractile vacuoles of *Dictyostelium amoebae*. J. Cell Biol. 121, 1311-1327.

Inouye, K., 1988. Differences in cytoplasmic pH and the sensitivity to acid load between prespore cells and prestalk cells of *Dictyostelium*. J. Cell Sci. 91, 109-115.

Inouye, K., 1988. Induction by acid load of tha maturation of prestalk cells in *Dictyostelium discoideum*. Development 104, 669-681.

Inouye, K., 1990. Control mechanism of stalk formation in the cellular slime mould *Dictyostelium discoideum*. Forma 5, 119-134.

Inouye, K., Gross, J., 1993. In vitro stalk cell differentiation in wild-type and slugger mutants of *Dictyostelium discoideum*. Development 118, 523-526.

Kay, R. R., Gadian, D. G., Williams, S. R., 1986. Intracellular pH in *Dictyostelium*: a $^{31}$P nuclear magnetic resonance study of its regulation and possible role in controlling cell differentiation. J. Cell Sci. 83, 165-179.

Khademi, S., O'Connell, J. 3rd, Remis, J., Robles-Colmenares, Y., Miercke, L. J., Stroud, R. M., 2004. Mechanism of ammonia transport by Amt/MEP/Rh: structure of AmtB at 1.35 A. Science 305, 1587-1594.

Kikuma, T., Ohneda, M., Arioka, M., Kitamoto, K., 2006. Functional analysis of the ATG8 homologue Aoatg8 and role of autophagy in differentiation and germination in *Aspergillus oryzae*. Eukaryot. Cell 5,1328-1336.

Kirisako, T., Baba, M., Ishihara, N., Miyazawa, K., Ohsumi, M., Yoshimori, T., Noda, T., Ohsumi, Y., 1999. Formation process of autophagosome is traced with Apg8/Aut7p in yeast. J. Cell Biol. 147, 435-446.

Kirsten, J. H., Xiong, Y. H., Dunbar, A. J., Rai, M., Singleton, C. K., 2005. Ammonium transporter C of *Dictyostelium discoideum* is required for correct prestalk gene expression and for regulating the choice between slug migration and culmination. Dev. Biol. 287, 146-156.

Kirsten, J. H., Xiong, Y., Davis, C. T., Singleton, C. K., 2008. Subcellular localisation of ammonium transporters in *Dictyostelium discoideum*. BMC Cell Biol. 9, 71.

Klaus, M., George, R. P., 1974. Microdissection of developmental stages of the cellular slime mold, *Dictyostelium discoideum*, using a ruby laser. Dev. Biol. 39, 183-188.

Kosta, A., Roisin-Bouffay, C., Luciani, M. F., Otto, G. P., Kessin, R. H., Golstein, P., 2004. Autophagy gene disruption reveals a non-vacuolar cell death pathway in *Dictyostelium discoideum*. J. Biol. Chem. 279, 48404-48409.

Kubohara, Y., Maeda, M., Okamoto, K., 1993. Analysis of the maturation process of prestalk cells in *Dictyostelium discoideum*. Exp. Cell Res. 207, 107-114.

Larsen, K. E., Sulzer, D., 2002. Autophagy in neurons: a review. Histol. Histopathol. 2002, 17, 897-908.

Levi, S., Polyakov, M., Egelhoff, T. T., 2000. Green fluorescent protein and epitope tag fusion vectors for *Dictyostelium discoideum*. Plasmid 44, 231-238.

Levine, B., Klionsky, D. J., 2004. Development by self-digestion: molecular mechanisms and biological functions of autophagy. Dev. Cell 6, 463-477.

Levraud, J. P., Adam, M., Luciani, M. F., de Chastellier, C., Blanton, R. L., Golstein, P., 2003. *Dictyostelium* cell death: early emergence and demise of highly polarized paddle cells. J. Cell Biol. 160, 1105-1114.

Ludewig, U., 2006. Ion transport versus gas conduction: function of AMT/Rh-type proteins. Transfus. Clin. Biol. 13, 111-116.

MacWilliams, H. K., Bonner, J. T., 1979. The prestalk-prespore pattern in cellular slime molds. Differentiation 14, 1-22.

Maeda, M., 1988. Dual effects of cAMP on the stabilty of prespore vesicles and 8-bromo cAMP-enhanced maturation of spore and stalk cells of *Dictyostelium discoideum*. Devel. Growth Differ. 30, 573-587.

Maeda, Y., and Takeuchi, I., 1969. Cell differentiation and fine structures in the development of the cellular slime molds. Devel. Growth Differ. 11, 232-245.

Maeshima, M., 2001. Tonoplast transporters: Organisation and Function. Annu. Rev. Plant Physiol. Plant Mol. Biol. 52, 469-497.

Marty, F., 1999. Plant vacuoles. Plant Cell 11, 587-600.

Neuhauser, B., Dynowski, M., Ludewig, U., 2009. Channel-like $NH_3$ flux by ammonium transporter AtAMT2. FEBS Lett. 583, 2833-2838.

Nolta, K. V., Steck, T. L., 1994. Isolation and initial characterisation of the bipartite contractile vacuole complex from *Dictyostelium discoideum*. J. Biol. Chem. 269, 2225-2233.

Otto, G. P., Wu, M. Y., Kazgan, N., Anderson, O. R., Kessin, R. H., 2003. Macroautophagy is required for multicellular developmentof the social amoeba *Dictyostelium discoideum*. J. Biol. Chem. 278, 17636-17645.

Otto, G. P., Wu, M. Y., Kazgan, N., Anderson, O. R., Kessin, R. H., 2004. *Dictyostelium* macroautophagy mutants vary in the severity of their developmental

defects. J. Biol. Chem. 279, 15621-15629.

Raper, K.,, Fennell, D. I., 1952. Stalk formation in *Dictyostelium*. Bull. Torrey Bot. Club 79, 25-51.

Rooney, E. K., Gross, J. D., 1992. ATP-driven $Ca^{2+}/H^{+}$ antiport in acid vesicles from *Dictyostelium*. Proc. Natl. Acad. Sci. USA 89, 8025-8029.

Schindler, J., Sussman, M., 1977. Ammonia determines the choice of morphogenetic pathways in *Dictyostelium discoideum*. J. Mol. Biol. 116, 161-169.

Shoji, J. Y., Arioka, M., Kitamoto, K., 2006. Vacuolar membrane dynamics in the filamentous fungus *Aspergillus oryzae*. Eukaryot. Cell 5,411-421.

Singleton, C. K., Zinda, M. J., Mykytka, B., Yang, P., 1998. The histidine kinase *dhkC* regulates the choice between migrating slugs and terminal differentiation in *Dictyostelium discoideum*. Dev. Biol. 203, 345-357.

Singleton, C. K., Kirsten, J. H., Dinsmore, C. J., 2006. Function of ammonium transporter A in the initiation of culmination of development in *Dictyostelium discoideum*. Eukaryot. Cell 5, 991-996.

Tang, N., Shi, J. L., Peng, J. T., Hou, L. S., 2006. Morphology of the apoptosis and cell differentiation during *Dictyostelium discoideum* development. Acta Zoologica Sinica 52, 603 - 611.

Tekinay, T., Wu, M. Y., Otto, G. P., Anderson, O. R., Kessin, R. H., 2006. Function of the *Dictyostelium discoideum* atg1 kinase during autophagy and development. Euk. Cell 5, 1797-1806.

Watts, D. J., Ashworth, J. M., 1970. Growth of myxameobae of the cellular slime mould *Dictyostelium discoideum* in axenic culture. Biochem. J. 119, 171-174.

Whittingham, W. F., Raper, K. B., 1960. Non-viability of stalk cells in *Dictyostelium*. Proc. Natl. Acad. Sci. USA 46, 642-649.

Williams, J. G., 2006. Transcriptional regulation of *Dictyostelium* pattern formation. EMBO Rep. 7, 694-698.

Yamamoto, A., Maeda, Y., Takeuchi, I., 1981. Development of an autophagic system in differentiating cells of the cellular slime mold *Dictyostelium discoideum*. Protoplasma 108, 55-69.

Yamamoto, A., Takeuchi, I., 1983. Vital staining of autophagic vacuoles in

differentiating cells of *Dictyostelium*. Differentiation 24, 83-87.

Yoshino, R., Morio, T., Yamada, Y., Kuwayama, H., Sameshima, M., Tanaka, Y., Sasaki, H., Iijima, M., 2007. Regulation of ammonia homeostasis by the ammonium transporter AmtA in *Dictyostelium discoideum*. Eukaryot. Cell 6, 2419-2428.

Zheng, L., Kostrewa, D., Berneche, S., Winkler, F. K., Li, X. D., 2004. The mechanism of ammonia transport based on the crystal structure of AmtB of Escherichia coli. Proc. Natl. Acad. Sci. USA 101,17090-17095.

**Figure legends**

Fig.1
Localisation of AmtA-GFP to the membranes of stalk-cell vacuoles. (A) Upper part of the stalk of a developing fruiting body of the AmtA-GFP transformant. Fluorescent (left) and DIC (right) confocal images are shown. Within the stalk tube (arrowheads), most cells have developed a single large vacuole (stalk-cell vacuole), and AmtA-GFP is located on their membranes. The cell-to-cell variability in fluorescence intensity is due to the unavoidable variability in the expression level of the introduced gene. (B) Sequential confocal images of a developing fruiting body of the AmtA-GFP transformant. Frames are shown at 10 minutes intervals. The cell indicated by the arrow had numerous fluorescent vesicles when it was at the entrance of the stalk tube, but develops a large vacuole with a fluorescent membrane. (C) Two AmtA-GFP cells each having a single stalk-cell vacuole. These cells were induced to differentiate into stalk cells *in vitro* by addition of 8-Br-cAMP. AmtA-GFP is predominantly localised to the membranes of stalk-cell vacuoles and weakly to the nuclear envelope (arrowheads). In migrating slugs, the AmtA-GFP fluorescence on the nuclear envelope was often more intense. (D) Sequential confocal images of an AmtA-GFP cell differentiating into a stalk cell *in vitro*. Fluorescence images were recorded at 30 seconds intervals (Movie 1), and frames are shown here at 10 minutes intervals. These large vesicles (numbered 1-3) fuse with the larger vesicle (4) to form a large vacuole. (E) Projected areas of the four vesicles in the cell shown in D. The projected areas (S) of the four vesicles were measured for all frames and plotted against time. Green: vesicle 1, red: vesicle 2, blue: vesicle 3 and yellow: vesicle 4. Open triangles indicate the sum of them. The area of vesicle 4 increases to a new level at every fusion event, and the increment is approximately equal to the area of the vesicle that fused with it (shown as the height of vertical bars of the corresponding colour). The dip in each graph around 14 minutes was due to defocusing of the cell, whereas the peak around 35 minutes seems to have been caused by the irregular shape changes of the vesicle. The first 6 frames in D correspond to 0, 10, 20, 30, 40, and 50 minutes on this graph. (F) Estimated total surface area (square) and volume (triangle) of the vesicles shown in D. Since the cell was not strongly flattened, the projected areas can be used as approximations of the surface area of the vesicles. The vesicles were assumed to be spherical and their centres to be on the focal plane, then the surface area of a vesicle can be calculated from its projected area S to be 4S, and its volume to be $(4/3)\ \pi^{-1/2}\ S^{3/2}$. The three vertical bars above the graph indicate the time of fusion events. There are sources of errors in this simplified estimation, such as movements of small vesicles in the z-direction, irregular shape of vesicles, particularly of the large ones, and

probable over-estimation of the volume of the large vacuole. In spite of these, a trend of the increase in the total volume with the relatively constant total surface area is evident. A, C and D are in the same magnification. Bars, 10 μm.

Fig. 2
Localisation of AmtA-GFP to the membranes of autophagosomes and acidic vesicles. (A) Immuno-electron micrograph of an AmtA-GFP cell starved for 8 hours. The cell was reacted with an anti-GFP antibody and visualised by the pre-embedding gold enhancement immunogold method. Colloidal gold particles are enriched on the membranes of vacuoles which appear to contain mitochondria (magenta arrows) and fragments of subcellular structures. Mitochondria in the cytosol (green arrows), autolysosomes (green arrowhead) and probable autophagosomes (magenta arrowhead) are indicated. (B) AmtA-GFP cells at growth phase were loaded with a cytosol marker TRITC-dextran by electroporation and examined with a confocal microscope. Top: soon after staining, middle: after 8 hours of incubation in buffer, bottom: after 8 hours of incubation in nutrient medium. It is only under starvation condition that rhodamine fluorescence accumulated in AmtA-GFP vesicles. Left: AmtA-GFP, centre: TRITC-dextran, right: merge. (C) AmtA-GFP cells at growth phase were stained with neutral red and examined with a confocal microscope after 8 hours of incubation in buffer. A small fraction of AmtA-GFP vesicles (arrow) were devoid of red fluorescence. (D) GFP-Atg8 cells at growth phase were stained with neutral red and examined with a confocal microscope after 20 hours of incubation in buffer. There is no overlap between GFP-Atg8 and neutral red, indicating that GFP-Atg8-expressing vacuoles are not acidic. (E) Cells expressing both AmtA-GFP and RFP-Atg8 were starved for 4 hours and examined with a confocal microscope. B-E are in the same magnification. Bars, A: 1 μm, B-E: 10 μm.

Fig.3
(A) Distribution of GFP-Atg8 in starved cells (left), slug cells (centre), and stalk cells (right). A DIC image of the stalk is also shown to the right. (B) Behaviour of GFP-Atg8-positive vesicles during stalk cell differentiation. Prestalk cells dissociated from slugs were induced to differentiate *in vitro* by addition of 8-Br-cAMP, and time-lapse imaging was performed at 60 seconds intervals with a confocal microscope (Movie 2). GFP-Atg8 was localised on the membranes of small vesicles, presumably autophagosomes, but not on the membranes of autolysosomes or stalk-cell vacuoles. (C) Behaviour of contractile vacuoles in a differentiating stalk cell. Prestalk cells expressing GFP-Rab11 were dissociated from slugs and induced to differentiate *in vitro*. Time-lapse imaging was performed at 30 seconds intervals with a confocal

microscope (Movie 3). Contractile vacuoles (arrows) repeat a contraction-expansion cycle independently of stalk-cell vacuole formation. (D) Middle part of a fruiting body expressing GFP-VatM (Movie 4). DIC (left) and fluorescent (right) confocal images are shown. The membranes of stalk-cell vacuoles show GFP fluorescence. (E) Enlarged sequential confocal images of the same fruiting body shown in D. Five frames from a time-lapse recording taken at 30 seconds intervals (Movie 5) are shown. In the stalk cells within the stalk tube, contractile vacuoles continue to be active (arrows) after the formation of large stalk-cell vacuoles (arrowhead). Bars, 10 μm.

Fig.4
Enlargement of vacuoles and cell expansion. (A) Excerpt from a time-lapse DIC images of a stalk-cell differentiating *in vitro* are shown at 30 minutes intervals. (B) Total projected areas of the whole cell shown in A (triangle), the vacuoles (open diamond) and the cytosol (square) were measured and plotted. In this experiment, because the cell was strongly flattened, the projected area will be approximately proportional to the volume. Bar, 10 μm.

Fig.5
Cell wall formation *in vitro*. (A) Cell wall formation during stalk cell differentiation. Prestalk cells dissociated from slugs were induced to differentiate *in vitro* in the presence of Calcofluor, and time-lapse imaging was performed at 60 seconds intervals with a fluorescence microscope. Left: phase contrast, right: Calcofluor fluorescence. Frames are shown at 40 minutes intervals (Movie 6). (B) Total vacuole volumes (square) and fluorescent intensity of the cell wall (circle) of the left cell in A were measured and plotted. Best fit sigmoid curves were calculated by the least square method. The vacuole volume stopped increasing after initiation of cell wall formation. Bar, 10 μm.

Fig.6
Schematic diagrams of an autolysosome in a prestalk cell (A) and a differentiating stalk cell (B). Only one autolysosome is shown in each figure for simplicity. The majority of acidic vesicles in prestalk cells have been shown to be autophagic vacuoles (autolysosomes), which are acidified by vacuolar $H^+$-ATPase. (A) High ammonia levels in migrating slugs prevent prestalk cells from differentiating into stalk cells, and this has been proposed to be due to the reduced acidification of acidic vesicles by the in-coming ammonia (Gross, 1994). In the model shown here, $NH_3$ from outside takes up $H^+$ to become $NH_4^+$ (1), while AmtA acts as a channel for $NH_3 + H^+$ (indicated as $NH_4^+$ in the figure), and their outflow through the channel (2) effectively results in

proton leakage (indicated by a grey arrow), which prevents excessive acidification of the autolysosome. (B) Upon a drop in external ammonia during culmination, $NH_3$ escapes from the autolysosome (3), causing a release of a large amount of protons from the accumulated $NH_4^+$ (4) within the autolysosome. This would enhance the hydrolytic activities and osmotic pressure of the autolysosome, resulting in its expansion. Loss of $NH_3$ from the cytosol (5), as well as inflow of weak acids from the neighbouring cells (not shown), also promote cytoplasmic acidification, which helps further acidification of the autolysosome (Inouye, 1990). The dotted arrows on the $H^+$-ATPase and AmtA indicate reduced transport due to the increased $H^+$ gradient and decreased $NH_4^+$ gradient, respectively, across the autolysosome membrane. In *amtA*-null mutant cells, $NH_4^+$ accumulates in autolysosomes because the channel (2) is absent. The resulting low pH condition in autolysosomes is equivalent to the low ammonia situation shown in B. It remains unknown whether and how other ammonium transporters affect the vacuolar pH, and they are not included in the model. Other important components affecting the vacuolar pH, such as $Ca^{2+}/H^+$ exchanger and plasma membrane $H^+$-ATPase are not shown.

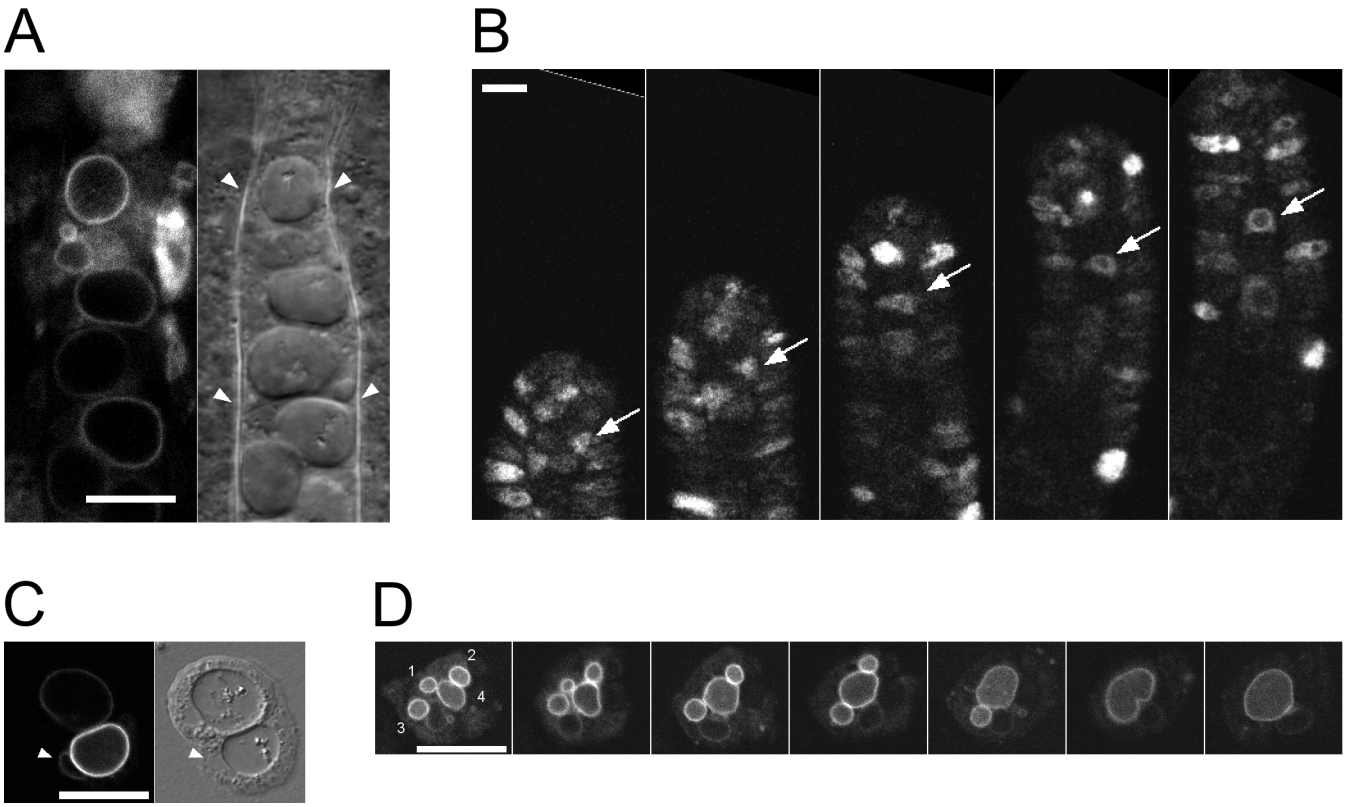
A
B
C
D
1
2
3
4
E
F
Projected area ( µm² )
Time (min)
Estimated volume ( µm³ )
Estimated surface area ( µm² )
Time (min)

Fig. 1

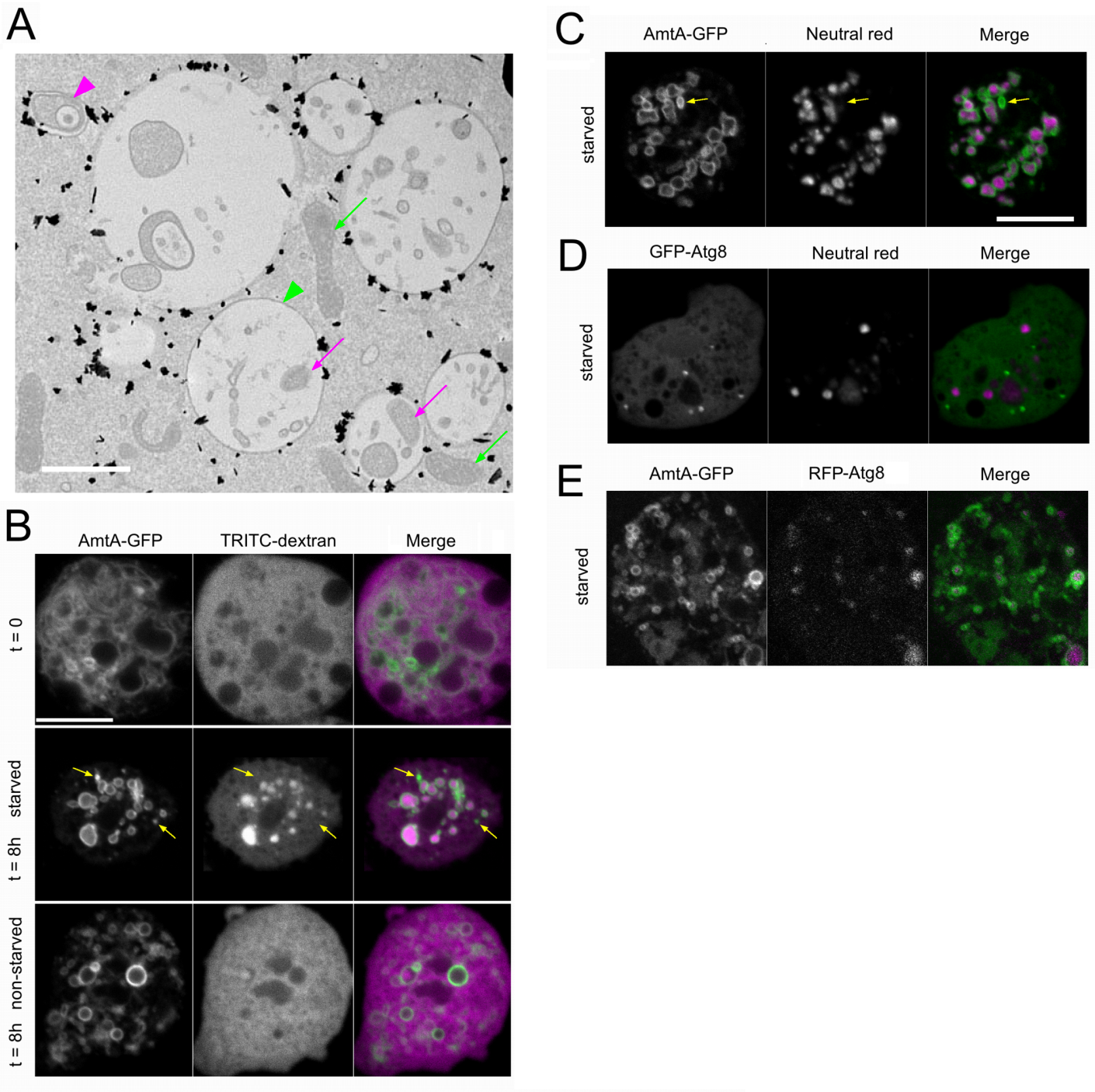
A
B
AmtA-GFP
TRITC-dextran
Merge
t = 0
t = 8h starved
t = 8h non-starved
C
AmtA-GFP
Neutral red
Merge
starved
D
GFP-Atg8
Neutral red
Merge
starved
E
AmtA-GFP
RFP-Atg8
Merge
starved

Fig. 2

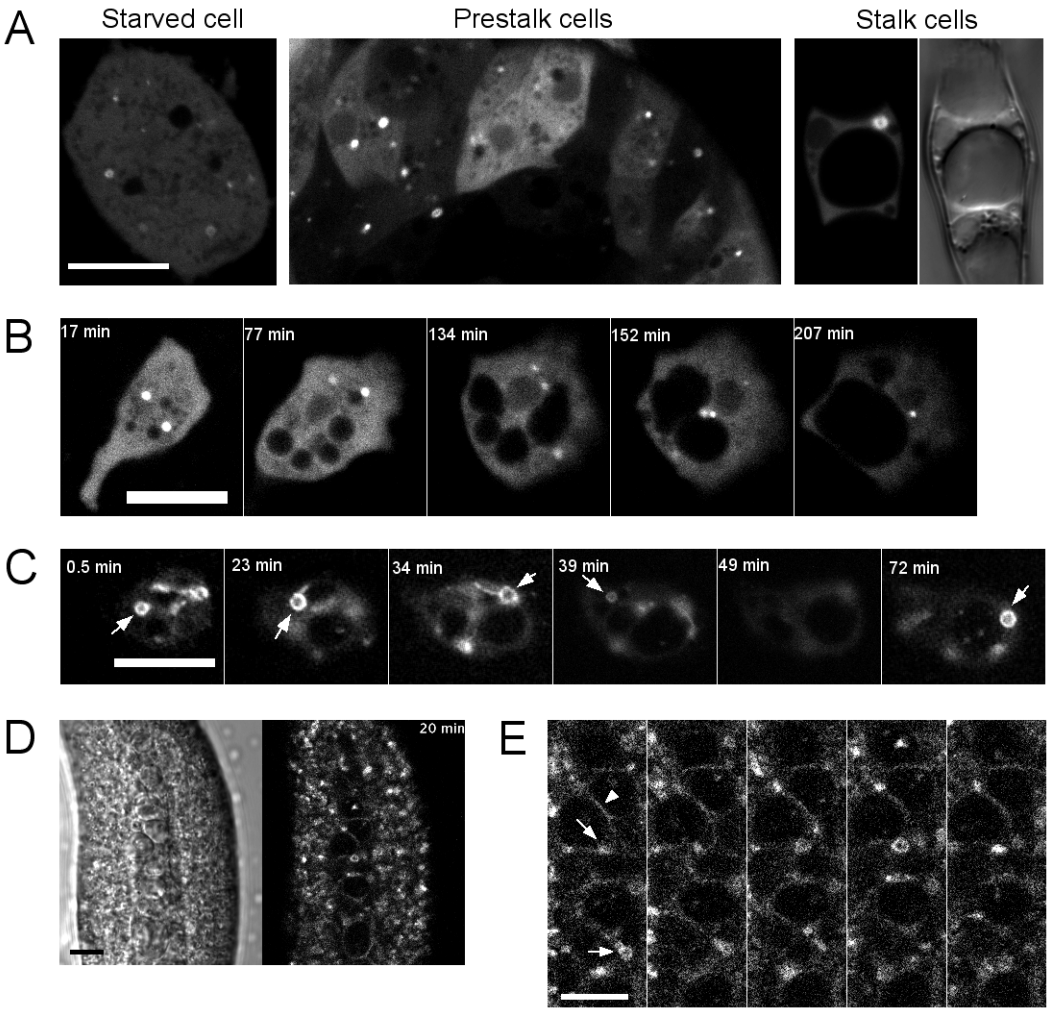
A
Starved cell
Prestalk cells
Stalk cells
B
17 min
77 min
134 min
152 min
207 min
C
0.5 min
23 min
34 min
39 min
49 min
72 min
D
20 min
E

Fig. 3

A

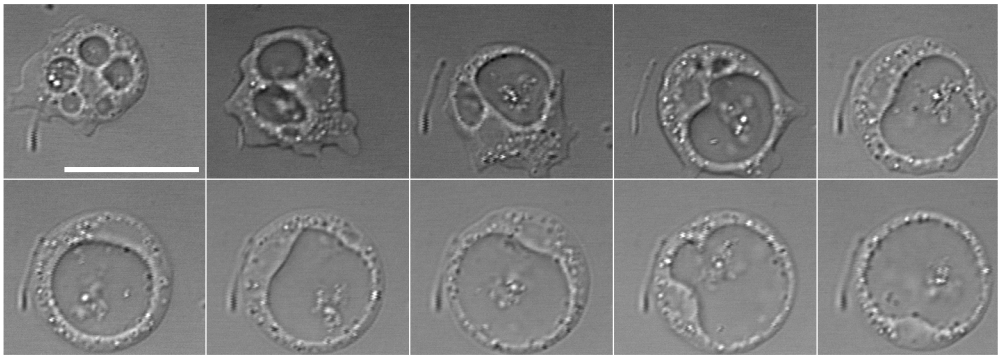

B

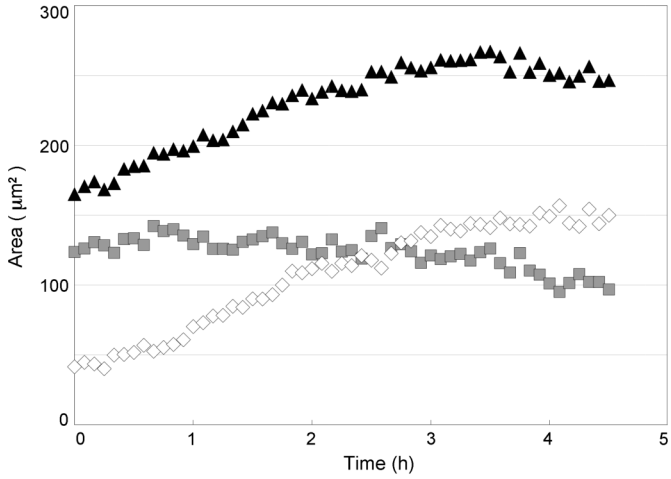


Fig. 4

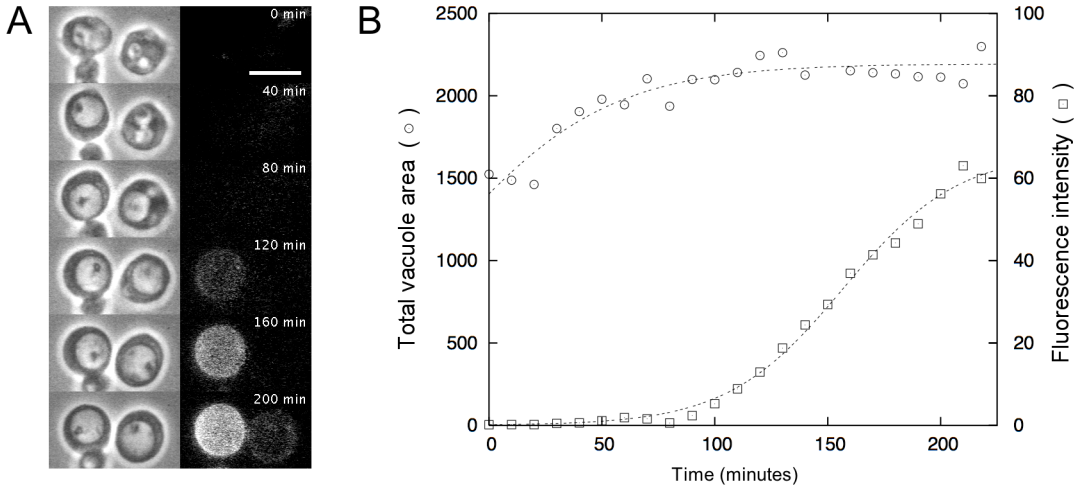
A
0 min
40 min
80 min
120 min
160 min
200 min
B
Total vacuole area ( ○ )
Fluorescence intensity ( □ )
Time (minutes)
2500
2000
1500
1000
500
0
100
80
60
40
20
0
0
50
100
150
200

Fig. 5

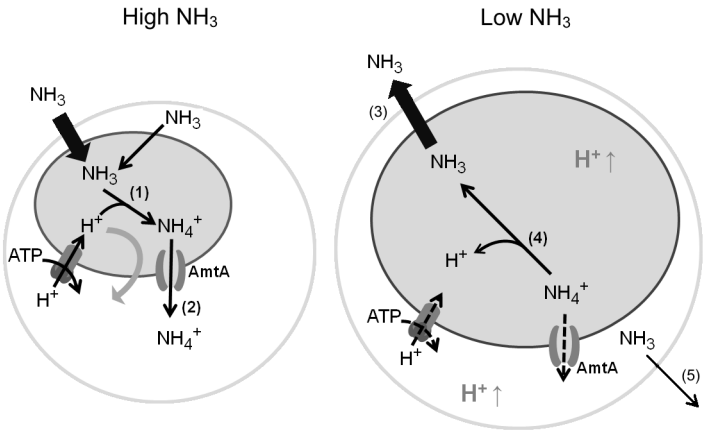
High NH3
Low NH3
NH3
NH3
NH3
(1)
H+
NH4+
ATP
H+
AmtA
(2)
NH4+
NH3
(3)
NH3
H+ ↑
(4)
H+
NH4+
ATP
H+
AmtA
NH3
(5)
H+ ↑

Fig. 6